The 2013 World Congress on
Advances in Structural Engineering and Mechanics (ASEM13)
Jeju, Korea, September 8-12, 2013

Effect of number of loading cycles on seismic behavior of steel tube-reinforced concrete composite columns

*Mingliang Zhang[1)], Xiaodong Ji[2)], Hongzhen Kang[3)], Jiaru Qian[4)]

[1), 2), 4)] Key Laboratory of Civil Engineering Safety and Durability of China Education Ministry, Department of Civil Engineering, Tsinghua University, Beijing 100084, China
[3)] Department of Civil Engineering, Tangshan College, Tangshan 063000, China

ABSTRACT

The steel tube-reinforced concrete (ST-RC) composite column is a novel type of composite column, which consists of a steel tube embedded in reinforced concrete. The objective of this paper is to investigate the effect of the number of loading cycles on seismic behavior of the ST-RC columns through experimental testing. Six large-scale ST-RC column specimens were subjected to high axial forces and lateral cyclic loading. The specimens included two groups, where Group I had higher amount of transverse reinforcement while Group II had relatively lower amount of transverse reinforcement. The test results indicate that all specimens failed in a flexural mode, characterized by buckling and yielding of longitudinal rebars, fracture of hoops and crossties, compressive crushing of concrete, and buckling of steel tube at the base of columns. The number of loading cycles was found to have minimal effect on the strength capacity of the specimens. The number of loading cycles had limited effect on the deformation capacity for the Group I specimens, while it obviously affected the deformation capacity for the Group II specimens. When ten cycles of lateral loading were repeated at each drift level, the Group I specimen showed obviously larger deformation and cumulative energy dissipation capacities than the corresponding Group II specimen. The ultimate displacement and failure displacement of the former were 25% and 41% larger than those of the latter, and the cumulative energy dissipated by the former was 2.8 times that of the latter. Allowing for the effect of cumulative damage of high-rise buildings subjected long-period ground motions; the recommendation is made on the requirements of the amount of transverse reinforcement for seismic design of ST-RC columns for ensuring adequate deformation capacity.

1. INTRODUCTION

Steel has the advantages of high strength and ductility in resisting tension and flexure, while concrete has the advantages of relatively high strength and stiffness in resisting compression. With a judicious combination of these two construction materials, the steel-concrete composite members can have the beneficial qualities of both materials. The steel tube-reinforced concrete (ST-RC) composite column is a novel type of composite column, which consists of a steel tube embedded in reinforced concrete (Lin 2002 and Lin 2008). In recent years, many efforts have been made on the studies of the behavior and design of the ST-RC columns, for example, Chen 2005, Nie 2005, Lin 2003, Cai 2002, Kang 2011, Zhao 1996, Qian 2009, Li 1998 and Han 2009. As a result,

the technical specification for steel tube-reinforced concrete column structure CECS188:2005 has published. Till now, the ST-RC columns have been used in China for more than forty buildings, showing both technical and economic benefits.

ST-RC columns are mainly used in high-rise buildings in regions of high seismicity. In the 2011 off the Pacific coast of Tohoku earthquake, many high-rise buildings in Tokyo experienced significant vibration with a duration of several minutes because of the resonance to the long-period ground motions (Takewaki 2011). In fact, the E-Defense shaking table tests on large-scale high-rise building models have shown that high-rise buildings could sustain large vibrations with a long duration when subjected to long-period motions (Chung 2010 and Ji 2011). Severe cumulative damage to the structural components might be induced by many cycles of inelastic deformations. Fig. 1 shows the time history of drift ratio in the second story of a twenty-one story steel frame structure subjected to a synthesized long-period motion, which was recorded by the E-Defense shaking table test. Ten cycles of vibrations were repeated at the lateral drift ratio of over 0.01 which is the limiting drift for a steel high-rise building under the design-based earthquakes.

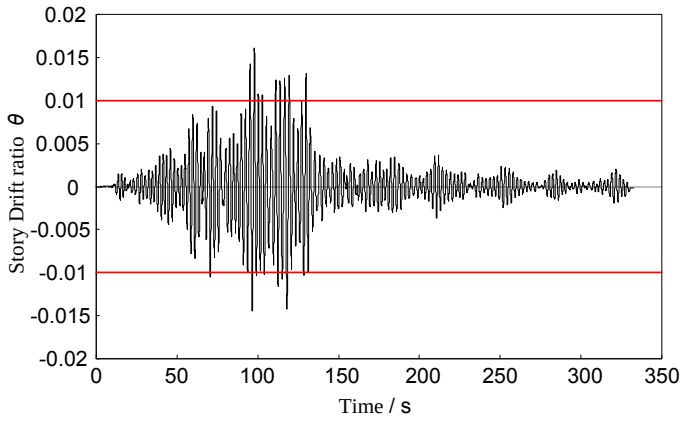

Fig 1. Time history of story drift ratio for high-rise building under long-period motion

In the past tests on the ST-RC columns, the lateral loads reversed two or three cycles at each drift level, which might not fully include the cumulative damage. Hence, those test results may overestimate the deformation capacity of the ST-RC columns if they are subjected to many cycles of lateral loadings (Kawashima 1988). Since the structural details for seismic design of ST-RC columns specified in CECS188:2005 are based on the past test data, these design details may not guarantee adequate deformation capacity if the ST-RC columns subjected to long-period, long-duration earthquake motions.

In this paper, the effects of numbers of loading cycles and of the amount of transverse reinforcement on seismic behavior of the ST-RC columns are investigated through quasi-static tests on six large-scale column specimens. The deformation capacity of the ST-RC columns when subjected to various loading histories is examined. In addition, the recommendation is made on the requirements of the transverse

reinforcement for seismic design of ST-RC columns for ensuring adequate deformation capacity.

2. TEST SPECIMENS

2.1 Specimen design

A total of six specimens labeled CC1 to CC6 were tested. The ST-RC column had a square cross-section of 500 mm by 500 mm, and a height of 2220 mm. The column was cast together with a reinforced concrete foundation beam, with which the specimen was clamped to the rigid reaction floor. Fig. 2 shows the sectional dimensions and reinforcement details of the specimens. Four D22 (diameter=22 mm) and eight D18 (diameter=18 mm) steel rebars were placed as the longitudinal reinforcement of the column, corresponding to an area ratio (i.e., the ratio of gross cross-sectional area of longitudinal rebars over that of the column) of approximately 1.4%. A steel tube with an outer diameter of 299 mm and a thickness of 7.4 mm was embedded in the center of the column section. The ratio of the cross-sectional area of concrete filled steel tube (CFST) core over that of the column was 0.28 for all specimens. The transverse reinforcement consisted of rectangular hoops and bent crossties. D8 (diameter=8 mm) steel rebars were used as transverse reinforcement. The thickness of concrete cover was 25 mm. The amount of transverse reinforcement was taken as one of major test variables.

The specimens can be categorized into two groups. Group I specimens (odd numbers in the nomenclature i.e., CC1, CC3, and CC5) had the stirrup with a spacing of 70 mm in vertical. Group II specimens (even numbers in the nomenclature i.e., CC2, CC4, and CC6) stirrup spacing were 100 mm. The specimens were designed to satisfy the “strong shear and weak bending” mechanism and the tests results showed that all specimens failed in a flexure mode. The column was cast together with a reinforced concrete foundation beam, with which the specimen was clamped to the rigid reaction floor.

Table1 Parameters of specimens

Specimen No.	Cubic strength (MPa)		Confinement index		Axial force ratio		Volumetric transverse reinforcement ratio (%)		Stirrup characteristic value	
	$f_{cu,m}$	$f_{c,t}$	ξ_d	ξ_t	n_d	n_t	$\rho_{v,1}$	$\rho_{v,2}$	$\lambda_{d,1}$	$\lambda_{d,2}$
CC1	50.1	38.1	1.60	1.03	0.72	0.39	1.30	2.03	0.18	0.29
CC2	50.1	38.1	1.60	1.03	0.72	0.39	0.91	1.42	0.13	0.20
CC3	48.8	37.1	1.60	1.06	0.72	0.40	1.30	2.03	0.18	0.29
CC4	48.8	37.1	1.60	1.06	0.72	0.40	0.91	1.42	0.13	0.20
CC5	52.2	39.7	1.60	0.99	0.72	0.38	1.30	2.03	0.18	0.29
CC6	52.2	39.7	1.60	0.99	0.72	0.38	0.91	1.42	0.13	0.20

Note: 1) Subscripts d and t represent the design and test values, respectively;
2) Subscript 1 and 2 represent that the volumetric transverse reinforcement ratio are calculated by

Methods 1 and 2, respectively.

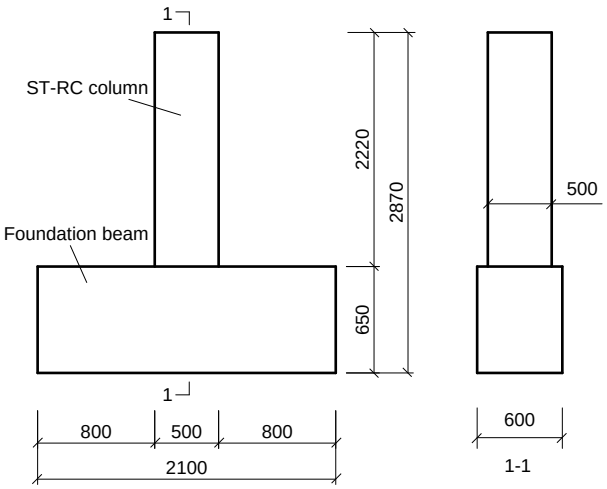

(a) Elevation view

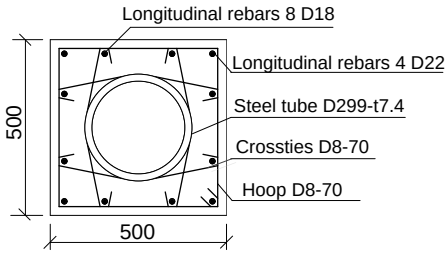

(b) Section dimensions and reinforcement details for Group I specimens: CC1, CC3, CC5

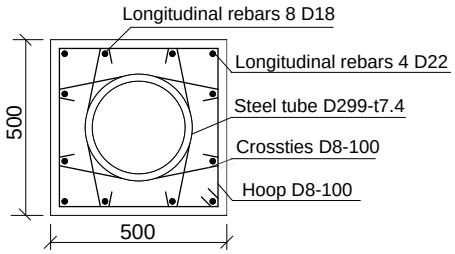

(c) Section dimension and reinforcement details for Group II: CC2, CC4, CC6

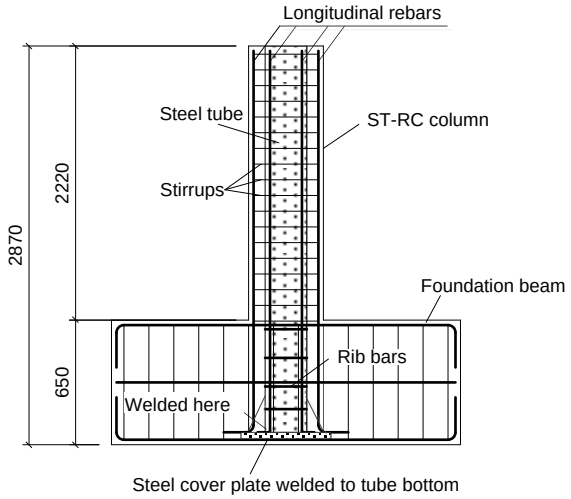

(d) Elevation view of steel tube and reinforcement

Fig.2 ST-RC column specimens

The outer and infilled concrete had a design strength grade of C45 (the nominal

cubic compressive strength, f_{cu} = 45 MPa, and the design value of axial compressive strength, $f_{c,d}$ = 21.1 MPa). Cubic compressive strength of the concrete was tested with cubes 150 mm in size and five cubes were tested for each type of concrete. The average cubic strengths of the concrete measured at the time of specimen testing are listed in Table 1. The measured axial compressive strength of concrete $f_{c,t}$ was taken as 0.76 times $f_{cu,m}$ for C45 grade concrete, in accordance with the Chinese code for design of concrete structures (GB 50010-2010); The design strength of the longitudinal reinforcement, D22 and D18 rebars, was 360 MPa. The design strength of the transverse reinforcement, D8 rebars, was 300 MPa. The yield strengths of the D22, D18 and D8 rebars measured by coupon tests were 451, 470 and 372 MPa, respectively. The steel tube were fabricated from Q345 steel (the design strength $f_{y,d}$ = 315 MPa), and their yield strength measured by coupon tests was 354 MPa.

Table 1 show the design and test values of the confinement index of the CFST core. The confinement index is defined as $\xi=f_aA_a/(f_{cc}A_{cc})$, where f_a denotes the strength of steel tube, f_{cc} denotes the axial compressive strength of infilled concrete, A_a and A_{cc} denote the cross-sectional areas of the steel tube and infilled concrete, respectively. Note that, the design strengths of materials were used to calculate the design value of the confinement index, while the measured strengths of materials were used to calculate the test value. The design value of the confinement index ξ_d for the CFST core was 1.6, and the test value was approximately 1.0.

(a) Method 1 (b) Method 2

Fig. 3 Volume of stirrup-confined concrete used in calculation of volumetric transverse reinforcement ratio

Table 1 also shows the volumetric transverse reinforcement ratio ρ_v (i.e., the ratio of the volume of the stirrups to that of the concrete confined by stirrups). Two methods were adopted to calculate the volume of the stirrup-confined concrete in calculation of the volumetric transverse reinforcement ratio. Method 1 uses the volume of all stirrup-confined concrete that includes the volume of the core CFST (as shown in Fig. 3 (a)), while Method 2 uses the volume of the stirrup-confined concrete outside of the steel tube (i.e., extracting the volume of the core CFST as shown in Fig. 3(b)) according to Technical Specification CECS 188:2005. The amount of transverse reinforcement is also expressed in terms of the stirrup characteristic value λ specified in GB 50011-2010 (i.e., the mechanical volumetric ratio specified in Euro Code 8). The stirrup characteristic value is calculated as $\lambda=\rho_v f_{yv}/ f_c$, where f_{yv} and f_c denote the yield strength of transverse

reinforcement and the axial compressive strength of the concrete, respectively. The design stirrup characteristic values for the Group I and II specimens were 0.18 and 0.13, respectively, if using the volumetric transverse reinforcement ratio calculated by Method 1. The design stirrup characteristic values for the Group I and II specimens were 0.29 and 0.20, respectively, if using the volumetric transverse reinforcement ratio calculated by Method 2.

The applied axial compressive load was 5300 kN for all specimen. For ST-RC columns, the axial force ratio was defined as follows:

$$n_{\mathrm{d}} = \frac{N_{\mathrm{d}}}{f_{\mathrm{co,d}}A_{\mathrm{co}} + 0.9f_{\mathrm{cc,d}}A_{\mathrm{cc}}(1+\alpha\xi_{\mathrm{d}})} \tag{1-a}$$

$$n_{\mathrm{t}} = \frac{N_{\mathrm{t}}}{f_{\mathrm{co,t}}A_{\mathrm{co}} + 0.9f_{\mathrm{cc,t}}A_{\mathrm{cc}}(1+\alpha\xi_{\mathrm{t}})} \tag{1-b}$$

in which, n denotes the axial force ratio; N denotes the axial load applied on the specimen; f_{co} and f_{cc} denote the axial compressive strength of the outer concrete and infilled concrete in the steel tube, respectively; A_{co} and A_{cc} denote the cross-sectional areas of the outer concrete and infilled concrete; ξ denotes the confinement index of the CFST; the coefficient α = 2.0; and subscripts d and t represent the design and test values, respectively. Note that the specified load factor (i.e., the ratio of design load to test load) is taken as 1.2 according to GB 50011-2010.

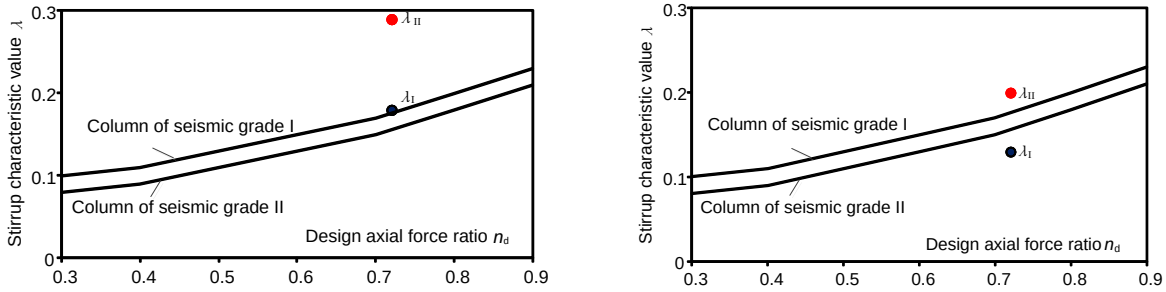

(a) Group I：CC1、CC3、CC5　　(b) Group II：CC2、CC4、CC6

Fig. 4 Design axial force ratio versus stirrup characteristic value of specimens

Table 1 presents the design value n_{d} and test value n_{t} of the axial force ratio. The design axial force ratio n_{d} was 0.72 for all specimens, and the test value n_{t} slightly varied from 0.38 to 0.40. Fig. 4 shows plots of the amount of transverse reinforcement versus design axial force ratios of the specimens. GB 50011-2010 specifies the lower limit of the amount of transverse reinforcement for ductile RC columns, which relates to their design axial force ratios. Fig. 4 also shows the requirement for the stirrup characteristic values specified by GB 50011-2010 for RC columns of seismic grade I (high ductile columns) and columns of seismic grade II (medium ductile columns). Fig. 4 indicates that if using Method 1 to calculate the stirrup characteristic value, the amount of transverse reinforcement of the Group I specimens satisfied the requirement for the

columns of seismic grade I, while the Group II specimens did not satisfy the requirement. If using Method 2, the stirrup characteristic value for the Group II specimens could satisfy the requirement on the amount of transverse reinforcement for the columns of seismic grade I.

2.2 Test setup, loading program and instrumentation

Fig. 5 shows the test setup, where the specimen was placed in a load frame. The foundation beam was securely clamped to the reaction floor. The top of the column was clamped to two hydraulic jacks, one in the horizontal direction and another in the vertical direction. The vertical jack could move freely in horizontal to accommodate the lateral displacement of the specimens. A vertical load was applied to the specimen initially and was maintained constantly for the duration of the test. Afterwards, cyclic loads were applied quasi-statically by the horizontal hydraulic jack. The horizontal loading point was 2000 mm above the base of the column. The shear-to-span ratio equaled to 4.0 for all specimens.

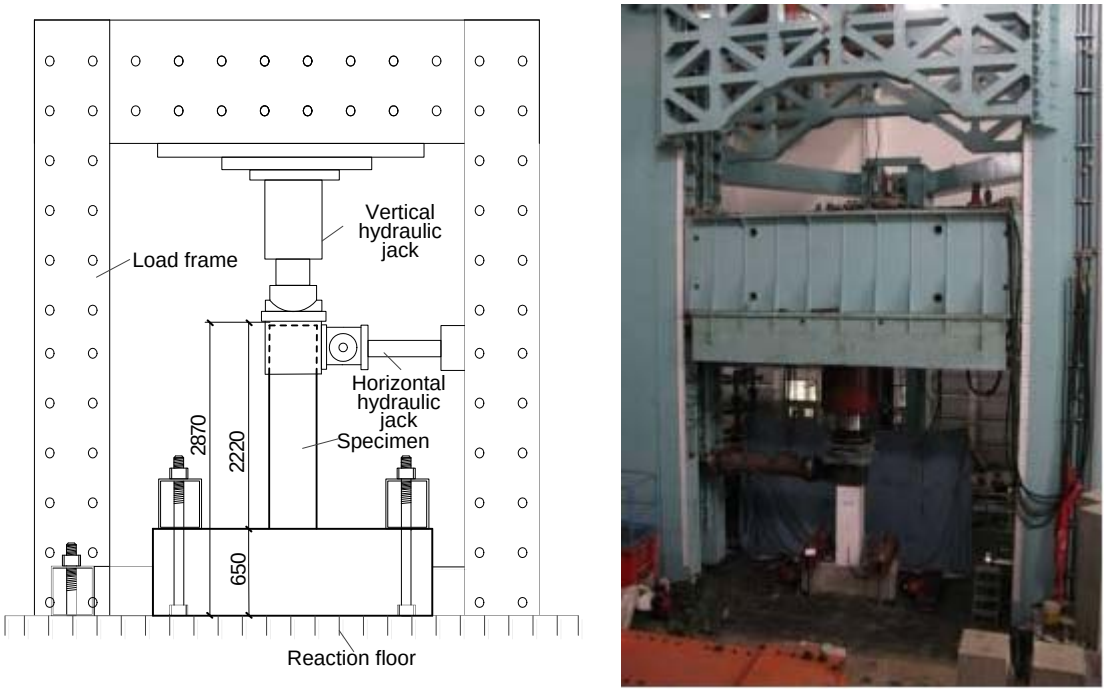

(a) Drawing (b) Photo

Fig.5 Test setup

Fig. 6 shows the history of lateral cyclic loading for the tests. The lateral loading was displacement-controlled, where the lateral displacement of the column top was monitored by the linear variable differential transformer (LVDT) $1^{\#}$, as shown in Fig. 7. The displacement was expressed in terms of the drift ratio θ, and the drift ratios increased in the sequence of 0.002, 0.0035, 0.005, 0.0075, 0.01, 0.015, 0.02, 0.025, 0.03, and 0.035. The specimens yielded at around 0.005 drift. One cycle was performed at each drift level before the specimen yielded. When the drift ratio arrived at 0.005,

multi-cycles were repeated at each drift level. To investigate the effect of numbers of loading cycles, different numbers of cycles were performed for different pairs of specimens. Three cycles were repeated for Specimens CC1 and CC2 at each drift level, five cycles for Specimens CC3 and CC4, and ten cycles for Specimens CC5 and CC6. In each loading cycle, a push was exerted first, followed by a pull, where the push was defined as the positive +ning. The test was terminated when the specimen lost their lateral load-carrying capacity, which was regarded as the complete failure of the column.

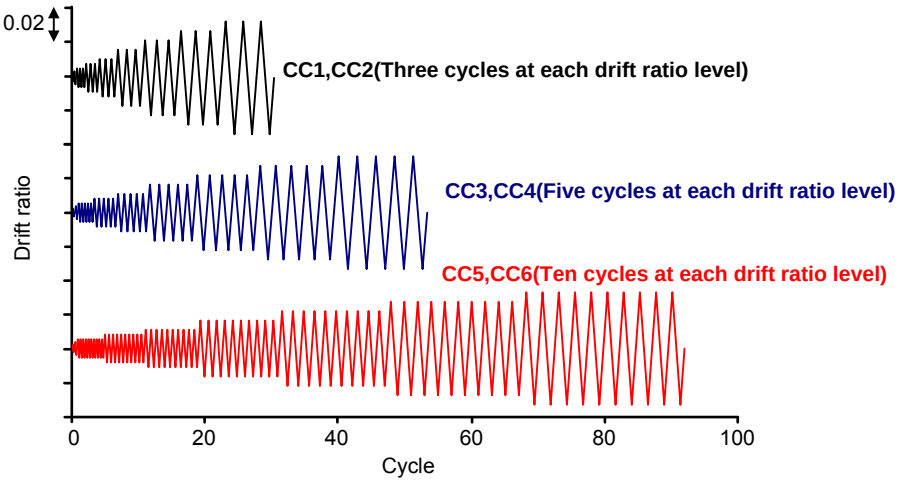

Fig.6 Loading history

Instrumentation was used to measure the loads, displacements and strains of the specimens. Load cells measured the vertical and lateral loads applied to the specimen. Fig. 7 shows the locations of the LVDTs and strain gauges mounted on the specimen. Four LVDTs (i.e., LVDTs 1$^{\#}$ through 4$^{\#}$) measured the lateral displacements along the height of the column. Six LVDTs (i.e., LVDTs 5 through 10) were mounted at the base of the wall to measure the local deformation from which the average vertical strains and the rotation in the plastic hinge region could be estimated. Three LVDTs (i.e., LVDTs 11$^{\#}$ through 13$^{\#}$) were mounted on the foundation beam, one used to monitor the horizontal slip of the foundation beam along the reaction floor and the other two used to monitor the rotation of foundation beam during the loading. Strain gauges were installed to measure the strains of the longitudinal rebars and steel tube. The Gauges were located 20 mm and 470 mm above the column base.

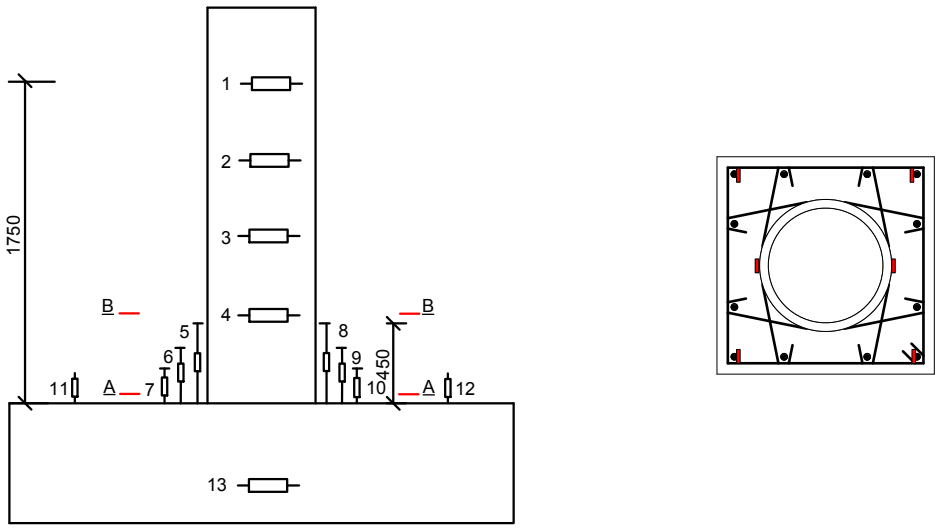

(a) LVDTs

(b) Strain gauges at Sections A-A & B-B

Fig.7 Specimen instrumentation

3. EXPERIMENTAL RESULTS

3.1 Damage and failure mode

The damage process of the specimens could be characterized by three stages: initial cracking stage, damage developing stage and failure stage. The observations at each stage are summarized below.

***Initial cracking stage*:** This stage began from the onset of testing to the occurrence of the initial crack. When the lateral drift ratio reached 0.005, a horizontal flexural crack was initially observed at the base of the column. Since the specimen was subjected to high axial force ratio, the longitudinal rebars approached to yield in compression at the initial cracking drift.

***Damage developing stage*:** This stage began from the initial cracking to the peak load of the specimens. Both the development of new cracks and the extending and widening of existing cracks were observed in this stage. The cracks were distributed in the region from the column base up to a height equal to approximately the column sectional depth. At 0.0075 drift, the longitudinal rebars in compression yielded. At 0.01 drift, slight vertical cracks caused by extremely large compressive strain developed at the corners of the column base, while the longitudinal rebars in tension and the steel tube did not yield yet. The residual drift ratio after unloading was 0.0015 in average for all specimens. Note that, the limiting drift ratio for the frame-shear walls interacting structures subjected to the maximum consideration earthquake is 0.01 (GB 50011-2010).

***Failure stage*:** This stage began from the peak load to the complete failure of the specimens. Table 2 shows failure process of the specimens. Concrete cover spalling occurred at further cycles. Afterwards, the longitudinal rebars buckled and hoops and crossties sustained fracture. Finally, significant crushing of the outer concrete and

buckling of the steel tube occurred, which led to the lost of lateral load-carrying capacity of the column. Note that, the core CFST could carry the vertical load applied to the column in the end of the testing.

Table 2 Failure process of specimens

Specimen No.	0.02 drift ratio	0.025 drift ratio	0.03 drift ratio	0.035 drift ratio
CC1	Spalling of concrete cover	Spalling of concrete cover	Buckling of longitudinal rebars	Buckling of longitudinal rebars, fracture of transverse rebars, crushing of outer concrete, buckling of steel tube
CC2	Spalling of concrete cover	Spalling of concrete cover	Buckling of longitudinal rebars, fracture of transverse rebars, crushing of outer concrete, buckling of steel tube	
CC3	Spalling of concrete cover	Spalling of concrete cover	Buckling of longitudinal rebars	Fracture of transverse rebars, crushing of outer concrete, buckling of steel tube
CC4	Spalling of concrete cover	Buckling of longitudinal rebars, fracture of transverse rebars, crushing of outer concrete, buckling of steel tube		
CC5	Spalling of concrete cover	Buckling of longitudinal rebars	Fracture of transverse rebars, crushing of outer concrete, buckling of steel tube	
CC6	Spalling of concrete cover, buckling of longitudinal rebars, fracture of transverse rebars, crushing of outer concrete, buckling of steel tube			

Table 2 indicates that the drift ratio at the instance when the specimen sustained complete failure decreased with an increase in the number of loading cycles. The drift at complete failure was 0.035, 0.035 and 0.03 for Specimens CC1, CC3 and CC5, respectively. The drift was 0.03, 0.025 and 0.02 for Specimens CC2, CC4 and CC6, respectively. It is also notable that the drift of the Group II specimen at complete failure

was smaller than that of the corresponding Croup I specimen.

The limiting drift ratio for the RC frame structure subjected to the maximum consideration earthquake is 0.02 (GB 50011-2010). Fig 8 shows the photographs of the specimens after 0.02 drift loading. At this instance, the residual lateral load-carrying capacity for Specimens CC1, CC2, CC3 and CC5 was over 70% of their lateral peak load, and the residual load-carrying capacity of Specimen CC4 was 65% of its peak load. However, Specimen CC6 sustained complete failure, with its lateral load-carrying capacity degrading to near zero.

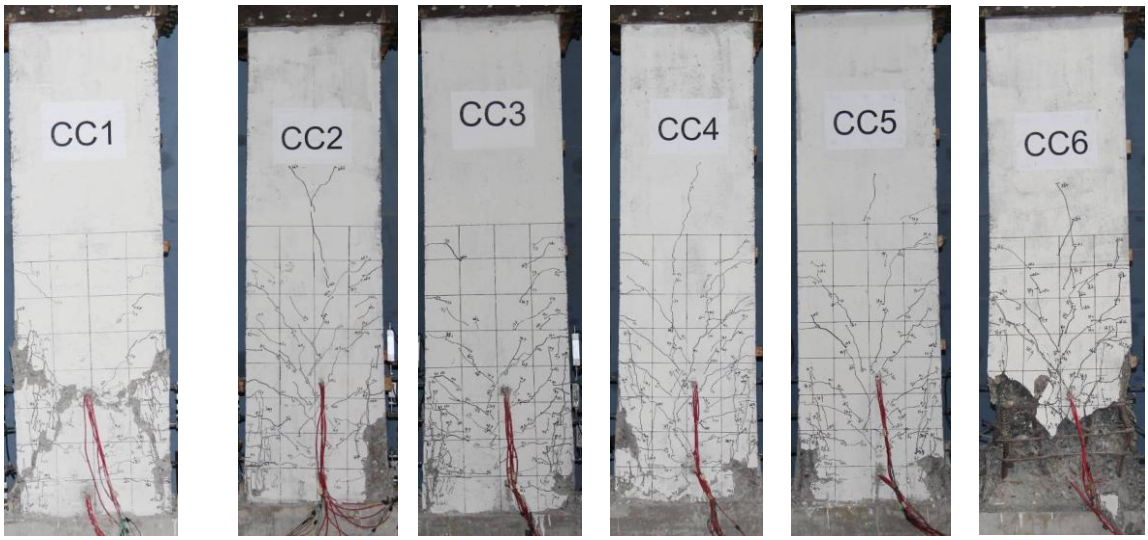

(a) CC1 (b) CC2 (c) CC3 (d) CC4 (e) CC5 (f) CC6

Fig. 8 Photographs of specimens after 0.02 drift loading

3.2 Force-displacement relationship

Fig. 9 shows the measured lateral force versus displacement relationship for all specimens. The hysteresis loops of all specimens were stable and not significantly pinched, showing the inherent good energy dissipation characteristics of ST-RC columns. Hysteresis loops of Group I specimens are fatter than Group II. Before the specimen arrived at its peak load, the hysteresis loops of different cycles at the identical drift were nearly identical. After the peak load, the strength degradation of different cycles at the identical drift became notable. The strength degradation of the Croup II specimen was more severe than that of the corresponding Group I specimen.

3.3 Lateral load-carrying capacity

Fig. 10 shows the lateral peak loads of the specimens. The peak load for the Group I specimens was around 620 kN except Specimen CC1, and that for the Group II specimens was approximately 580 kN. The numbers of loading cycles appears to have minimal effect on the lateral load-carrying capacity of the ST-RC columns. The smaller peak load of Specimen CC1 than other specimens was suspicious of being induced by non-compactness of concrete casting of CC1.

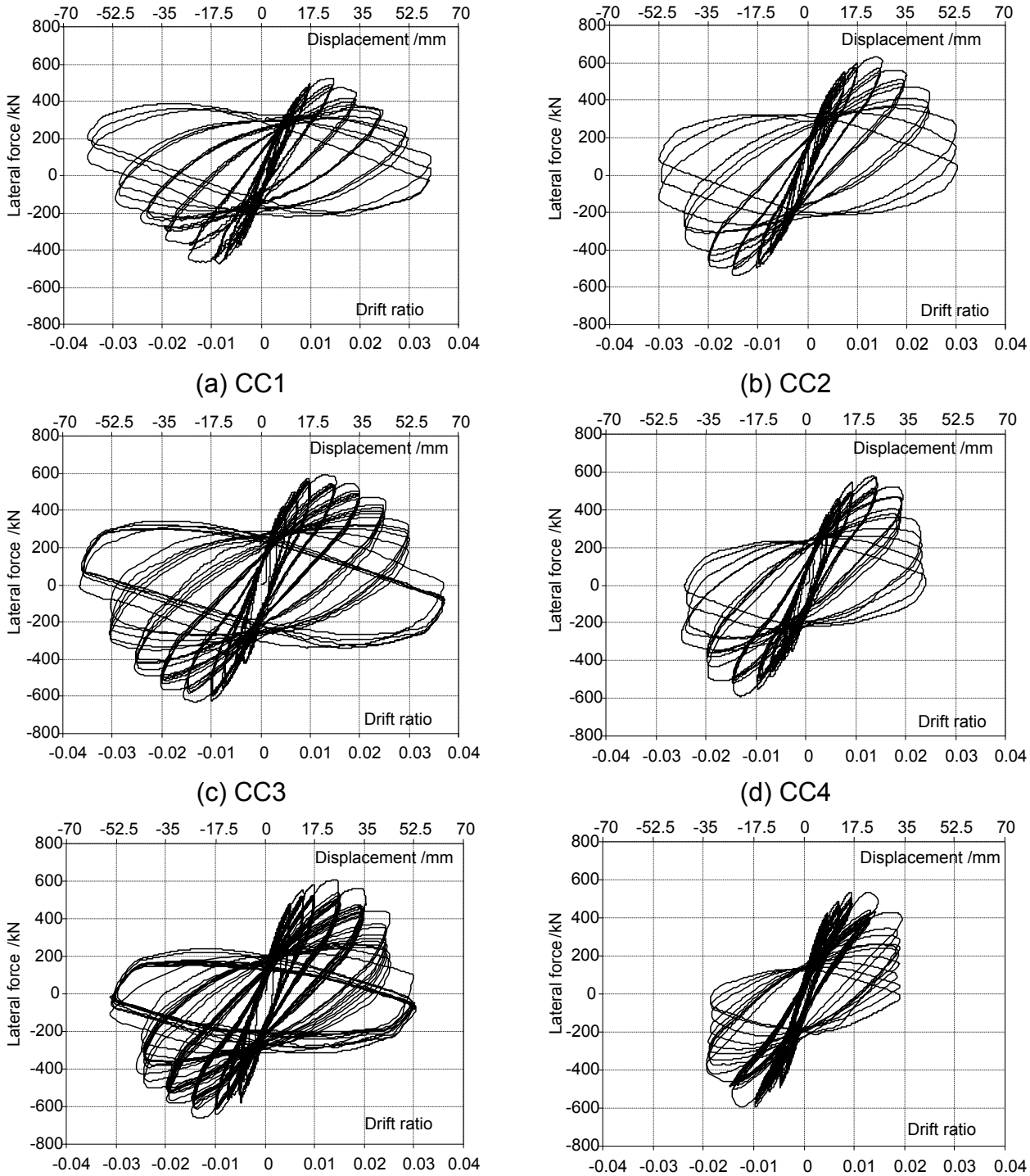

(a) CC1 (b) CC2

(c) CC3 (d) CC4

(e) CC5 (f) CC6

Fig.9 Hysteretic loops of lateral force versus displacement relationships of specimens

The average peak load of the Group I specimens (except for CC1) was 6% larger than that of the Group II specimens, indicating that the increasing amount of transverse reinforcement made limited increase of the flexural strength of the ST-RC columns.

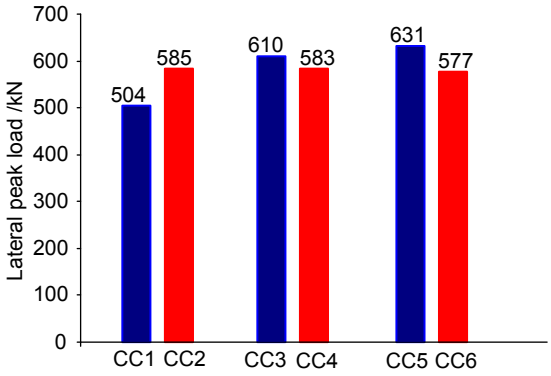

Fig.10 Peak load of specimens

4. DEFORMATION CAPACITY

Table 3 presents the yield displacement Δ_y, ultimate displacement Δu, failure displacement Δ_f, and their corresponding drift ratios. The yield displacement Δ_y was defined by using the concept of equal plastic energy. The ultimate displacement Δ_u was defined as the post-peak displacement at the instant when the lateral load decreases to 85% of the peak lateral load. The failure displacement Δ_f was defined as the post-peak displacement at the instant when the lateral load decreases to 50% of the peak lateral load. Note that all specimens except CC6 had stable hysteresis loops before Δ_f.

Table 3 Deformation capacity of specimens

Specimens No.	Yield		Ultimate		Failure	
	Disp. Δ_y (mm)	drift ratio θ_y	Disp. Δ_u (mm)	Drift ratio θ_u	Disp. Δ_f (mm)	Drift ratio θ_f
CC1	11.25	0.0064	31.85	0.018	47.36	0.027
CC2	12.85	0.0073	35.60	0.020	48.06	0.027
CC3	10.00	0.0057	38.00	0.022	52.81	0.030
CC4	11.30	0.0065	33.40	0.019	41.77	0.024
CC5	9.00	0.0051	37.45	0.021	47.21	0.027
CC6	9.85	0.0056	29.90	0.017	33.43	0.019

Since Specimen CC6 sustain complete failure before its envelope curve of lateral force-displacement relationship dropped to 50% of the peak load, its failure displacement was defined as the maximum loading displacement. The drift ratio was calculated by as $\theta=\Delta/H$, where H was the height of the LVDT 1# relative to the column base. Note that the values shown in Table 3 were calculated using the average values of the displacements measured in the push and pull directions.

4.1 Effect of number of loading cycles

Fig. 11 shows the envelope curves of lateral force versus drift ratio relationship of the specimens, where the lateral force is normalized by dividing the peak load. All the specimens had nearly identical initial stiffness. Before the peak load, the envelope curves of Specimens CC3 and CC5 were nearly identical, and those of CC2 and CC4 were similar. However, Specimen CC6 had a smaller drift at the peak load than Specimens CC2 and CC4. After the peak load, the strength of the specimens decreased more rapidly along with the increasing number of loading cycles. Table 3 indicates that the ultimate displacement and failure displacement of Specimens CC5 were 5% and 11% smaller than Specimen CC3. The effect of the number of loading cycles on the deformation capacity for the Group I specimens was not significant. However, for the Group II specimens, the ultimate displacement of Specimens CC4 and CC6 were 6% and 16% smaller than that of Specimen CC2, and the failure displacement of CC4 and CC6 were 13% and 30% smaller than that of Specimen CC2. Therefore, the effect of the number of loading cycles on the deformation capacity for the Group II specimens appeared to be significantly.

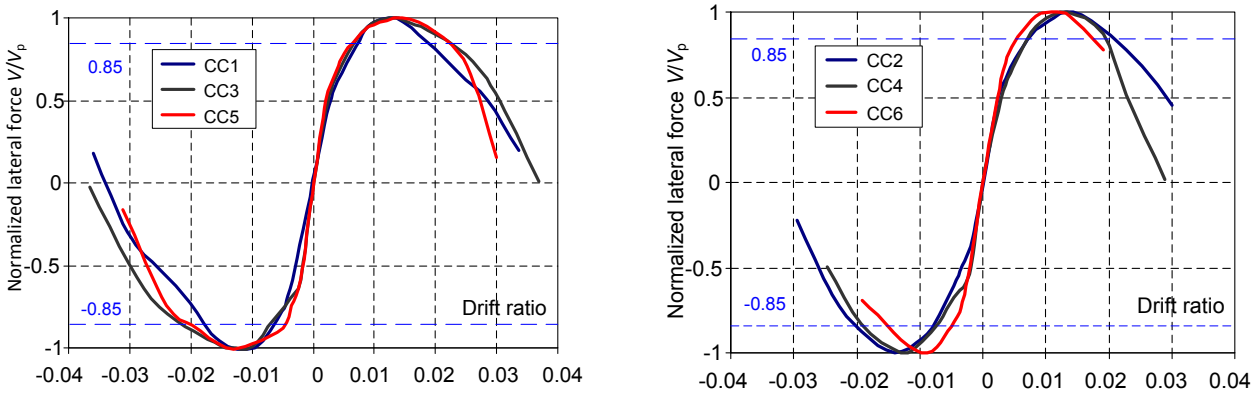

(a) Group I (b) Group II

Fig.11 Envelope curves of normalized lateral force versus drift ratio relationship of specimens: Effect of number of loading cycles

4.2 Effect of amount of transverse reinforcement

Fig. 12 shows the envelope curves of lateral force versus drift ratio relationship of specimens, which is used to show the effect of the amount of transverse reinforcement. For Specimen CC3 and CC4 that were loaded five cycles at each drift level, the ascending branches of their envelope curves were nearly identical, while Specimen CC4 showed more rapid strength decrease than CC3 after the peak load. For Specimens CC5 and CC6 that were loaded ten cycles at each drift level, Specimen CC6 had a smaller drift ratio at the peak load relative to CC5 because of severe cumulative damage. Meanwhile, Specimen CC6 had faster strength drop than CC5.

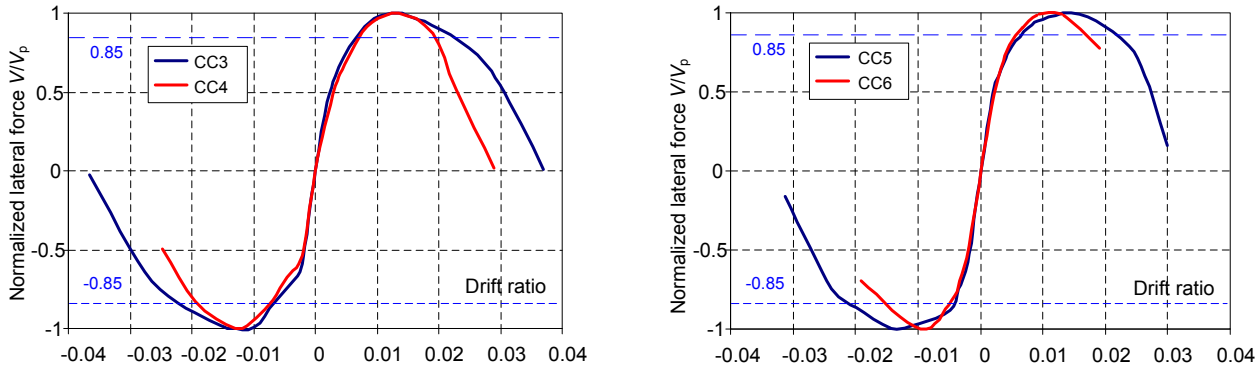

(a) CC3 versus CC4 (b) CC5 versus CC6

Fig.12 Envelope curves of normalized lateral force versus drift ratio relationship of specimens: Effect of amount of transverse reinforcement

Table 3 indicates that the ultimate drift and failure drift ratio of Specimen CC3 were 13% and 26% larger than those of CC4, respectively. The ultimate drift and failure drift of Specimen CC5 were 25% and 41% larger than those of CC6, respectively. For the Group I specimens, the ultimate drift was over 0.02 and the failure drift ratio was more than 0.025, even when the lateral cyclic loads repeated five or ten cycles at each drift. For the Group II specimens, the ultimate drift achieved 0.02 and the failure drift was over 0.025, if the number of loading cycles equaled to three. However, with five or ten loading cycles, the ultimate drift ratio was less than 0.02 and the failure drift ratio was less than 0.025.

Since the outer concrete is located at the edge of the section, where the strain is largest among the section under the combined axial force and bending moment, it sustained the most severe damage among the section. Accordingly, the cumulative damage performance of the ST-RC column is primarily related to the behavior of the outer concrete. Increased confinement to concrete could improve the cyclic behavior of the concrete. Fig. 13 shows the hysteresis loops of the lateral force versus vertical strain of plastic hinge for Specimens CC5 and CC6, where the vertical strain was calculated by the measured local deformation from the column base up to the height of 450 mm. Vertical strain of Specimen CC5 was stable in the ten loading cycles at 0.02 drift. However, the compressive plastic strain of Specimen CC6 was significantly developed in the loading cycles at 0.02 drift, which is attributed to the less confinement provided by the transverse reinforcement. This phenomenon also correlated well with the test observation that the concrete crushing was more rapid under cycle loading if the spacing of the transverse rebars. As the steel tube could not provide confine to the outer concrete, the transverse reinforcement for the ST-RC columns should be designed based on the volume of all stirrup-confined concrete for ensuring the good confinement to the outer concrete.

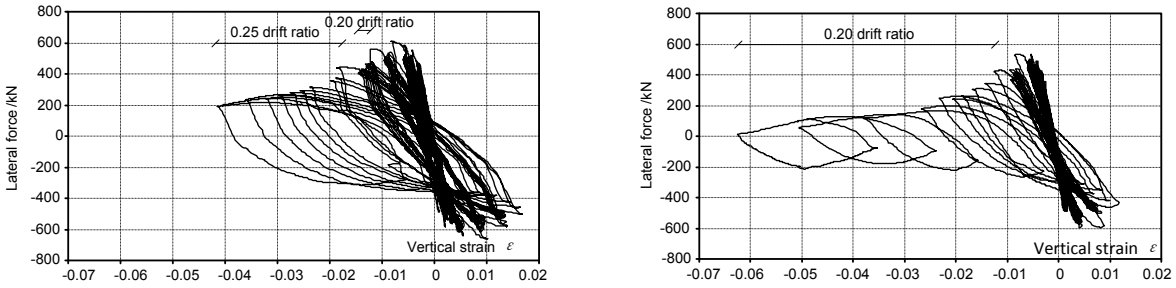

(a) CC5 (b) CC6

Fig.13 Hysteresis loops of lateral force versus vertical strain of plastic hinge of specimens

5. ENERGY DISSIPATION CAPACITY

The energy dissipated in a loading cycle equaled to the area surrounded by the corresponding hysteresis loop. Fig. 16 shows the cumulative energy dissipated by the specimens. The cumulative energy dissipation is defined as the sum of the energy dissipated by the stable hysteresis loops before the failure displacement Δ_f. Fig. 14 indicates that the cumulative energy dissipated by the Group I specimens (except for CC1) was significantly larger than that of the Group II specimens. The cumulative energy dissipation for Specimen CC3 and CC5 were 3.0 and 2.8 times that of Specimens CC4 and CC6, respectively, because the former had larger failure displacement than the latter. Although the increasing amount of transverse reinforcement did not increase the energy dissipated in each loading cycle, it could improve the cumulative energy dissipation capacity by increase of the displacement capacity.

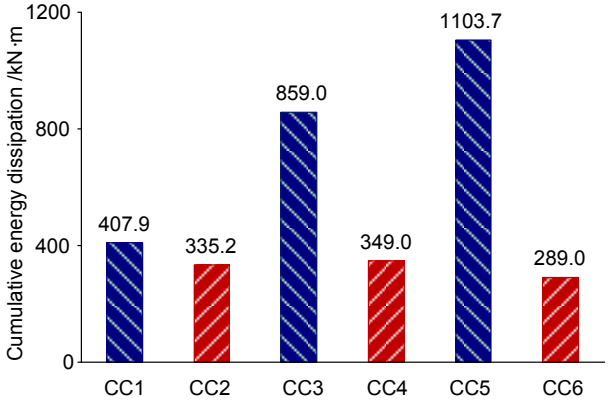

Fig.14 Cumulative energy dissipated by specimens

6. CONCLUSIONS

A series of quasi-static tests on six large-scale ST-RC columns were carried out to examine their seismic behavior and to study the effect of numbers of loading cycles. Major findings obtained from the study are as follows:

(1).The ST-RC column specimens showed a flexural failure mode, characterized by yield and buckling of longitudinal rebars, fracture of transverse rebars, compressive

crushing of concrete, and buckling of steel tube at the plastic hinge of columns.

(2).The number of loading cycle made a small difference on the lateral load-carrying capacity, while it affected the behavior of the columns after the peak load. With an increase in the number of loading cycles, the strength dropped more rapid, and the drift of the specimen at the complete failure decreased.

(3).The number of loading cycles had limited effect on the deformation capacity for the ST-RC column specimens (Group I) of which the transverse reinforcement was designed based on the volume of all stirrup-confined concrete, while it obviously affected the deformation capacity for the counterpart specimens (Group II) of which the transverse reinforcement was designed based on the volume of the stirrup-confined concrete outside of the steel tube.

(4).The Group I specimens showed larger deformation capacity than the corresponding Group II specimens. When the lateral cyclic loads repeated five cycles at each drift level, the ultimate drift and failure drift of the Group I specimens were 13% and 26% larger than those of the Group II specimens, respectively. When the cyclic loads repeated ten cycles at each drift level, the ultimate drift and failure drift of the Group I specimens were 25% and 41% larger than those of the corresponding Group II specimens, respectively.

(5).The Group I specimens had significantly larger cumulative energy dissipation capacity than the Group II specimens. The total cumulative energy dissipated by the former was around 2.8 times that of the latter.

(6).Allowing for the effect of cumulative damage of structures subjected to ground motions, the recommendation is made that the transverse reinforcement for the ST-RC columns should be designed based on the volume of all stirrup-confined concrete for ensuring adequate deformation capacity of the columns.

ACKNOWLEDGEMENTS

The work presented in this paper was sponsored by the National Natural Science Foundation of China research (Grants No. 51261120377 and No. 51008173) and by Tsinghua University Initiative Scientific Research Program (Grants No. 2012THZ02-1 and No. 2011THZ03). The writers wish to express their sincere gratitude to the sponsors.

REFERENCES

Lin, L. and Li, Q. (2002). “Composition of concrete and steel promotes the development of high-rise building.” *Journal of Southeast University*, Vol. **32**(5), 702-705 (in Chinese).

Lin, L. and Li, Q. (2008). “Design concept and analysis of technical economy for steel tube-reinforced concrete column.” *Building Structure*, Vol. **38**(3), 17-21 (in Chinese).

Chen, Z., Zhao, D., Yi, W. and Lin, L. (2005). “Experimental research on behavior of high strength concrete column reinforced with concrete-filled steel tube under axial compression.” *Journal of Dalian University of Technology*, Vol. **45**(5), 687-691(in Chinese).

Nie, J., Bai, Y., Li, S., Zhao, J. and Xiao, Y. (2005). “Analyses on composite column with inside concrete filled steel tube under axial compression.” *China Civil Engineering Journal*, Vol. **38**(9), 9-13 (in Chinese).

Lin, Y., Cheng. W. and Li, J. (2003). “Experiment and study of SRC columns with steel circle pipe subjected to axial compressive loading.” *Building Science Research of Sichuan*, Vol. **29**(4): 11-13 (in Chinese).

Cai, J., Xie, X., Yang, C., He, J. and Chen. H. (2002). “An experimental research on the composite column with core of high-strength concrete filled steel tube under axial compression loading.” *Journal of South China University of Technology*, Vol. **30**(6), 81-85 (in Chinese).

Kang, H. and Qian, J. (2011). „Experimental study on axial compressive capacity of high strength concrete-filled steel tube composite columns.“ *Building Structur*e, Vol. **41**(6), 64-67 (in Chinese).

Zhao, G., Zhang, D. and Huang, C. (1996). “Study of earthquake resistant behavior of high strength concrete column reinforced with concrete filled steel tube.“ J*ournal of Dalian University of Technology*, Vol. **36**(6), 759-766 (in Chinese).

Qian, J. and Kang, H. (2009). ,“Experimental study on seismic behavior of high-strength concrete-filled steel tube composite columns.“ *Journal of Building Structures*, Vol. (4), 88-96 (in Chinese).

Li, H., Wu, B. and Lin, L. (1998). “Study on seismic properties of laminated column with high strength concrete containing steel tube.” *Earthquake Engineering and Engineering Vibration*, Vol. **18**(1), 45-53 (in Chinese).

Han, L., Liao, F., Tao, Z. and Hong, Z. (2009). “Performance of concrete filled steel tube reinforced concrete columns subjected to cyclic bending.” *Journal of Constructional Steel Research*, Vol. **65**(8-9), 1607-1616.

CECS 188: 2005. “Technical specification for steel tube-reinforced concrete column structure.” Beijing: China Planning Press, 2005 (in Chinese).

Takewaki, I., Murakami, S., Fujita, K., Yoshitomi, S. and Tsuji, M. (2011).”The 2011 off the Pacific coast of Tohoku earthquake and response of high-rise buildings under long-period ground motions.” *Soil Dynamics and Earthquake Engineering*, Vol. **31**(11), 1511-1528.

Chung, Y., Nagae, T., Hitaka, T. and Nakashima, M. (2010). “Seismic resistance capacity of high-rise buildings subjected to long-period ground motions: E-Defense shaking table test.” *Journal of Structural Engineering* (ASCE), Vol.**136** (6): 637-644.

Ji, X., Fenves, G. L., Kajiwara, K. and Nakashima, M. (2011). “Seismic damage detection of a full-scale shaking table test structure.” *Journal of Structural Engineering* (ASCE), Vol. **137**(1),14-21.

Kawashima, K. and Koyama, T. (1988). “Effect of number of loading cycles on dynamic characteristics of reinforced concrete bridge pier columns.” *Structural Engineering/ Earthquake Engineering*, Vol. **5**(1), 183-191.

GB 50011-2010. “Code for seismic design of buildings.” Beijing: China Architecture & Building Press, 2010 (in Chinese).

GB 50010-2010. “Code for Design of Concrete Structures” Beijing: China Ministry of Construction, 2010 (in Chinese).